Robust Design of LCL-Filters for Active Damping in Grid Converters

Alzola, Rafael Pena; Liserre, Marco; Blaabjerg, Frede; Yang, Yongheng

Published in:
Proceedings of the 39th Annual Conference of the IEEE Industrial Electronics Society, IECON 2013

DOI (link to publication from Publisher):
10.1109/IECON.2013.6699311

Publication date:
2013

Document Version
Early version, also known as pre-print

Citation for published version (APA):
Alzola, R. P., Liserre, M., Blaabjerg, F., & Yang, Y. (2013). Robust Design of LCL-Filters for Active Damping in Grid Converters. In *Proceedings of the 39th Annual Conference of the IEEE Industrial Electronics Society, IECON 2013* (pp. 1248-1253). IEEE Press. Proceedings of the Annual Conference of the IEEE Industrial Electronics Society https://doi.org/10.1109/IECON.2013.6699311

Robust Design of LCL-Filters for Active Damping in Grid Converters

Peña-Alzola, Rafael; Liserre, Marco; Blaabjerg, Frede; Yang, Yongheng

Published in:
Proc. IEEE IECON 2013

DOI (link to publication from Publisher):
10.1109/IECON.2013.6699311

Publication date:
2013

Robust Design of *LCL*-Filters for Active Damping in Grid Converters

Rafael Peña-Alzola, Marco Liserre, Frede Blaabjerg, Yongheng Yang
Department of Energy Technology
Aalborg University
Potoppidanstraede 101, Aaborg DK-9220, Denmark
rpa@et.aau.dk, mli@et.aau.dk, fbl@et.aau.dk, yoy@et.aau.dk

***Abstract*—Grid converters require a simple inductor or an *LCL*-filter to limit the current ripples. The *LCL*-filter is nowadays the preferred solution as it allows lower inductance values. In order to solve the stability concerns, active damping is preferred to passive damping since it does not use dissipative elements. However, large variations in the grid inductance and resonances arising from parallel converters may still compromise the system stability. This calls for a robust design of *LCL*-filters with active damping. This paper proposes a design flow with little iteration for two well-known methods, namely lead-lag network and current capacitor feedback. The proposed formulas for the resonance frequency, grid and converter inductance ratio, and capacitance of the *LCL*-filter allow calculating all the *LCL*-filter parameters. An estimation for the achieved Total Harmonic Distortion (THD) of the grid current is also provided. Experimental results show very robust designs to the parameter variations.**

I. Introduction

Grid converters supply sinusoidal currents and use a simple inductor (i.e., an *L*-filter) or an *LCL*-filter to limit the current ripple. Using an *LCL*-filter results in lower inductance values and thus allowing a more compact design and lower losses. Because of these advantages, this solution is nowadays widespread used in distributed generation systems (e.g., solar and wind power systems) [1], [2]. The current control in a closed loop may result unstable due to the *LCL*-filter resonance. Passive damping solves this issue by using simple resistors, and consequently results in additional losses [3]. Active damping modifies the control algorithm without using dissipative elements [1]. A vast amount of literature on active and passive damping of *LCL*-filters is available [3]–[13].

The variations in the resonance frequency, due to weak grids with large inductance variations, may compromise the system stability [14]. Moreover, the increasing connection of grid converters in parallel has raised new stability problems because of the new appearing resonances. It has been shown in [15] that when connecting converters in parallel with very similar characteristics, the resultant equivalent grid inductance is multiplied by the number of converters. Hence, these situations call for a robust design of the *LCL*-filter to solve the stability concerns.

In view of this, a simple design procedure for *LCL*-filters with little iteration is proposed in this paper. The *LCL*-filter is intended to be adopted with two well-known active damping methods, namely lead-lag network and current capacitor feedback. Formulas to select all the *LCL*-filter parameters are provided. Analysis in the *z*-plane is utilized to demonstrate the stability and the robustness to the parameter variations. This paper is organized as follows: § II makes a succinct review of the control for the *LCL*-filter based grid converters. Focuses are put on the considerations for the *LCL*-filter design in § III, followed by the proposed design flow, which is illustrated in § IV. The experiments are provided in § V to verify the analysis, and finally the conclusions are presented in § VI.

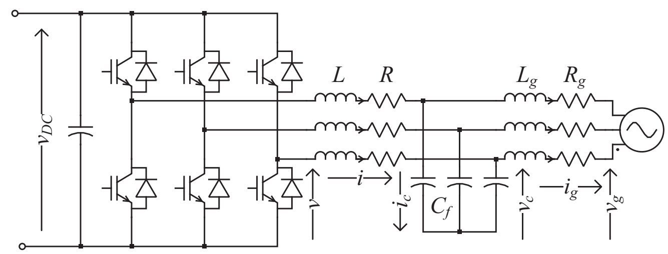

Fig. 1. An *LCL*-filter based three-phase active rectifier.

II. Control of the *LCL*-Filter Based Grid Converters

An *LCL*-filter based three-phase active rectifier is shown Fig. 1. For the power range of kilowatts (kW) to megawatts (MW), the current sensors are usually integrated in the converter for protection [5]. In this paper the converter side current is the one sensed for the control. The case of the grid current control is also analogous and simpler, since it is closer to the stability [16].

The cascaded control used for grid converters is represented in Fig. 2. The synchronization with the grid voltage is obtained by using a Phase-Locked Loop (PLL). The current control in the *dq*-frame uses simple Proportional-Integral (PI) controllers tuned according to the technical optimum criterion [17]. The *d*-axis current performs the DC voltage regulation whereas the *q*-axis current controls the reactive power. In the low frequency region, the *LCL*-filter behaves approximately as an equivalent *L*-filter resulting from neglecting the capacitor branch [5]. Therefore, the usual formulas for tuning the controllers in the *L*-filter case [17] can also be used in the *LCL*-filter case.

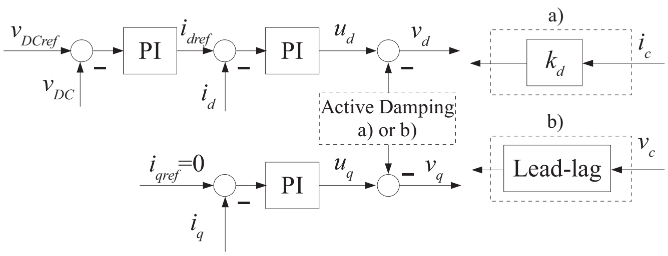

Fig. 2. Cascaded control of the grid converter with active damping: a) capacitor current feedback and b) lead-lag network.

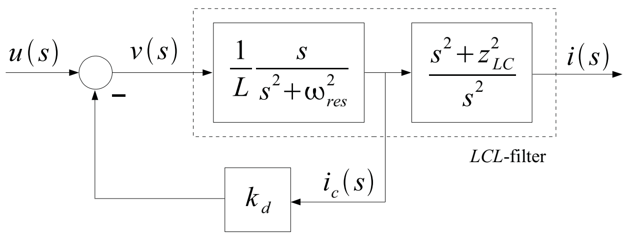

Fig. 3. *LCL*-filter with capacitor current feedback for active damping.

III. Considerations for the *LCL*-Filter Design

The block diagrams for the active damping methods of the lead-lag network and the capacitor current feedback have also been presented in Fig. 2.

A. Resonance Frequency

The capacitor current feedback, as it is shown in Fig. 3, result in damping for the *LCL*-filter.

The transfer function relating the converter current i and the converter voltage v can be expressed as [18]:

$$G_{ad}(s) = \frac{i(s)}{v(s)} = \frac{1}{Ls}\frac{\left(s^2 + z_{LC}^2\right)}{s^2 + 2\underbrace{\left[\frac{k_d}{2L\omega_{res}}\right]}_{damping}\omega_{res}s + \omega_{res}^2}, \quad (1)$$

where L and L_g are the inductances of the converter and grid inductors, respectively, $\omega_{res}^2 = (2\pi f_{res})^2 = (1 + L_g/L)z_{LC}^2$ is the resonance frequency with $z_{LC}^2 = [L_g C_f]^{-1}$, and finally C_f is the filter capacitance.

The digital implementation of the capacitor current feedback incorporates lag phase shifts due to the computational delay and the Pulse Width Modulation (PWM), as it is shown in Fig. 4.

The PWM for control modeling purposes is equivalent to a Zero-Order Hold (ZOH) [19]. In the s-domain, the transfer function modeling the effects of the computational delay and the PWM can be given as [15]:

$$G_d(s) = e^{-T_s s}\frac{1 - e^{-T_s s}}{T_s s}, \quad (2)$$

in which $T_s = 1/f_s$ is the sampling period. The pure delay in the first product of (2) models the the computational delay,

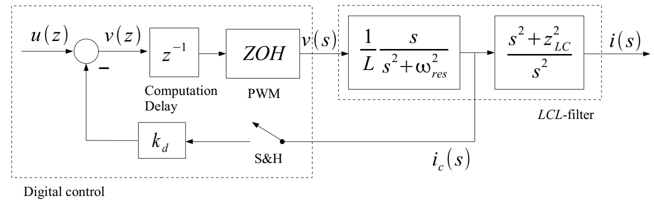

Fig. 4. Digital implementation of the capacitor current feedback.

while the second product models the ZOH [20]. The effects of the computation delay and the PWM at the resonance frequency can be studied by substituting $s = j\omega_{res}$ in (2):

$$G_d(j\omega_{res}) = e^{-T_s j\omega_{res}}\frac{1 - e^{-T_s j\omega_{res}}}{jT_s\omega_{res}}, \quad (3)$$

which can be factorized as,

$$G_d\left(j\omega_{res}\right) = \frac{\sin\left(\omega_{res}\frac{T_s}{2}\right)}{\omega_{res}\frac{T_s}{2}}e^{-j\omega_{res}\frac{3T_s}{2}}. \quad (4)$$

It gives an easy access to the magnitude and the phase of (2) at the resonance frequency.

For the case of $\omega_{res} = \pi/(1.5T_s)$, (3) or (4) results a negative number, which is equal to:

$$G_d(j\omega_{res}) = -\frac{3\sqrt{3}}{2\pi}. \quad (5)$$

The digital implementation delays at the resonance frequency, where damping is necessary, can be compensated by simply inverting (5). Thus, the ratio between the resonance frequency and the sampling frequency $r_f = f_s/f_{res}$ for active damping with the capacitor current feedback should be:

$$r_f = 3. \quad (6)$$

For the general case, the gain k_d times the real part of (2) at the resonance frequency should be positive:

$$k_d \Re\left\{e^{-T_s j\omega_{res}}\frac{1 - e^{-T_s j\omega_{res}}}{jT_s\omega_{res}}\right\} > 0. \quad (7)$$

Therefore, according to (7), the gain k_d should be negative when the real part of (2) at the resonance frequency is negative. This happens up to the maximum ratio $r_f = 6$. For higher r_f the real part of (2) is positive, k_d must be positive to fulfill (7), and in this case the computational and PWM delays can be considered negligible. The minimum ratio should be $r_f = 2$ as the sampling frequency should be higher than the resonance frequency so the resonance is visible for the digital control. Even though the previous approximations required assuming $f_{res} \ll f_s$, applying the Jury's criterion [6] to the digital implementation of the capacitor current feedback results in the same ratios r_f and the same signs for k_d. When considering the capacitor current feedback, the Padé approximant can be adopted as an equivalent model for the low frequency region

$\omega \ll \omega_{res}$, and it can be given as:

$$G_{adlf}(s) = \frac{i(s)}{u(s)} = \frac{1}{(L + L_g - R_g^2 C_f + k_d C_f R_g)s + (R + R_g)}, \quad (8)$$

in which R and R_g are the resistances of the converter and grid inductors respectively. This is almost the same as neglecting the capacitor branch in the *LCL*-filter since the additional terms are very small. It has been shown in [7] that the minimum k_d to obtain stability is:

$$k_{dmin} = \frac{1}{3} L_g f_s. \quad (9)$$

In [6], the transfer function of (1) is discretized and the maximum gain k_d resulting in stable poles is calculated. This value can be used as upper bound for k_d so it should not be higher than:

$$k_{dmax} = \frac{2}{3} \frac{\pi}{\sqrt{3}} L f_s. \quad (10)$$

The proper k_d will be selected by means of root locus analysis in the *z*-plane and considering the converter current control in a closed loop.

It has been shown in [7] that the ratio between the resonance and sampling frequency for the lead-lag network to work properly should be $r_f \approx 3.2 \div 3.4$. The minimum damping resistor for stability is approximately proportional to $R_d \propto f_s L_g^2/(L + L_g)$ and the capacitor harmonic current to $i_h \propto v_{DC}/(f_s L)$ with v_{DC} being the *DC*-link voltage [4]. With some simple calculations, the damping losses are approximately proportional to

$$P_d \propto \frac{(C_f v_{DC}^2 f_s)}{r_f^2}. \quad (11)$$

Therefore, for elevated r_f, passive damping should be considered as the damping losses will be very low. Finally, for grid current control with $r_f < 6$ [16], no active damping method is necessary to achieve stability.

B. Ratio between the Grid and Converter Inductance

For a constant ω_{res}, the ratio between the grid and converter inductances $r_l = L_g/L$ that minimizes the total inductance $L_T = L + Lg$:

$$L_T = \frac{1}{\omega_{res}^2} \frac{1}{C_f} \frac{(1 + r_l)^2}{r_l}, \quad (12)$$

is $r_l = 1$ (i.e., $L = L_g$) by deriving (12) and equating it to zero. This is equivalent to consider the minimal required capacitor [21]. In addition, equal inductors may result economically advantageous. Moreover, the ratio $r_l = 1$ also corresponds to the maximum attenuation for the main switching harmonics:

$$\frac{i_g(\omega_{sw})}{v(\omega_{sw})} = \frac{(1 + r_l)^2}{L_T \omega_{sw}(r_l^2 - C_f L_T r_l \omega_{sw}^2 + 2r_l + 1)}, \quad (13)$$

with $\omega_{sw} = 2\pi f_s$ by deriving again (13) and equating to zero. The ratio r_l influences the per unit variation of ω_{res} related to the per unit variation of the *LCL*-filter inductance according to the following:

$$\frac{\frac{d\omega_{res}}{\omega_{res}}}{\frac{dL_g}{L_g}} = -\frac{1}{2} \frac{1}{1 + r_l}, \quad (14a)$$

$$\frac{\frac{d\omega_{res}}{\omega_{res}}}{\frac{dL}{L}} = -\frac{1}{2} \frac{r_l}{1 + r_l}. \quad (14b)$$

Increasing r_l results in increased robustness to the grid inductance variations L_g according to (14). The detrimental effect for the converter inductance robustness is not problematic as L is a known parameter and not likely to vary. However, the value of r_l should not be increased very much to prevent the filter becoming too expensive being reasonable $r_l < 2$ [5]. The ratio r_l has no effect in the per unit variation of the *LCL*-filter capacitor, C_f:

$$\frac{\frac{d\omega_{res}}{\omega_{res}}}{\frac{dC_f}{C_f}} = -\frac{1}{2}, \quad (15)$$

and thus robustness to the resonance frequency because of capacitor variations can only be increased by increasing the capacitance C_f.

C. Capacitance of the LCL-Filter

Considering the converter current control equal to the rated current I_n synchronized to the capacitor voltage, approximately equal to the rated voltage V_n, the per unit value of the grid impedance results:

$$z_g = \frac{v_g}{i_g} = \frac{1}{1 + c_f^2} + j \left[\frac{c_f}{1 + c_f^2} - l_g \right] \approx 1 + j(c_f - l_g), \quad (16)$$

with lower letter indicating per unit values. The calculation of the grid impedance for other cases can be found in [22]. In order to make the grid impedance resistive, c_f should be equal to l_g according to (16). Substituting (16) in (12) results

$$c_f = \sqrt{1 + r_l} \frac{r_f \omega_n}{\omega_s}, \quad (17)$$

with $\omega_n = 2\pi f_f$ being the fundamental frequency and $\omega_s = 2\pi f_s$. However, (17) may result in very low capacitance and too high values for the inductances. Too large inductances results in large and expensive coils and no substantial advantage of the *LCL*-filter when compared to the simple *L*-filter. In order to reduce the value of the inductances, the capacitance should be increased but not to produce too much reactive power [22].

D. Estimation for the THD of the Grid Current

A lower bound for the RMS value of the capacitor current, based on the negligible impedance path in the capacitor branch, has been established in [4] and can be given as follows:

$$\tilde{i}_c^{low} = \frac{1}{2\sqrt{3}} \frac{1}{\sqrt{48}} \frac{v_{DC}}{f_{sw} L} \sqrt{\frac{3}{2} m^2 - \frac{3\sqrt{3}}{\pi} + \frac{9}{8} \left(\frac{3}{2} - \frac{9}{8} \frac{\sqrt{3}}{\pi} m^4 \right)} \quad (18)$$

where m is the modulation index and v_{DC} is the *DC*-link voltage. Equation (18) assumes using space vector modulation, and for other modulations [18] can be consulted. An upper bound for the RMS value of the capacitor current, by assuming negligible current harmonic for order $m_f - 6$ with $m_f = f_{sw}/f_f$ and f_f being the fundamental frequency, has also been established in [4] and can be expressed as:

$$\tilde{i}_c^{up} = \tilde{i}_c^{low} \left| \frac{s^2}{s^2 + \omega_{res}^2} \right|_{s=j((m_f-6)\omega_f)}. \qquad (19)$$

An upper bound for the RMS value of the grid current can be obtained by considering the transfer function relating i_g and i_c again at the harmonic order $m_f - 6$:

$$\tilde{i}_g^{up} = \tilde{i}_c^{up} \left| \frac{i_g(s)}{i_c(s)} \right|_{s=j((m_f-6)\omega_f)} = \tilde{i}_c^{up} \frac{z_{LC}^2}{((m_f-6)\omega_f)^2}. \qquad (20)$$

Even though an upper bound the estimation, (20) results optimistic when considering the voltage drops and conduction resistances of the power devices, dead-time and *DC*-link voltage ripples. Dividing (20) by the rated current I_n results approximately in the THD of the grid current.

IV. Step-by-Step Design Procedure for the *LCL*-Filter

The design flow for the *LCL*-filter is shown in Fig. 5 and is explained by means of an example. The grid converter has rated power $S_n = 4.1$ kW, rated voltage $V_n = 380$ V and switching frequency $f_{sw} = 8$ kHz. The selected active damping method is the capacitor current feedback with $r_f = 3$, and the impedance ratio, $r_l = 1$ (i.e., $L = L_g$). The capacitance according to (17) $C_f = 1.4$ μF would result in too large inductors. Selecting $C_f = 2.6$ μF (5%) will not produce very much reactive power and will result in $L = L_g = 2.7$ mH.

Fig. 6 shows the root locus in the *z*-plane for the closed loop system by varying k_d. The systems results stable for gains greater than $k_d = 7.25$, which is very close to $k_{dmin} = 7.28$ according to (9). The gain for the maximum damping shown in Fig. 6 is $k_d = 24.6$ a little lower than the maximum $k_{dmax} = 26.4$ in (10). It can be seen that the damping for the resonance poles can be selected at will by increasing the gain k_d. This is analogous to what happens with passive damping by increasing the resistor value [3].

Damping the resonance poles too much is not appropriate as it would result in too much control effort, a damping factor equal to $\zeta = 0.1$ is adequate [3]. Simulations using Matlab/Simulink and considering ideal power devices and passive elements result in a grid current THD equal to 0.51%. This is coherent with the upper bound for the grid current THD according to (20) equal to 0.65%. Fig. 7 shows the root locus in the *z*-plane for varying L_g from 40% to 1000%. The system remains stable for the full variation range. Hence, the proposed procedure for the capacitor current feedback results very robust to the grid inductance variations. Analysis in the *z*-plane for the lead-lag method can be found in [7].

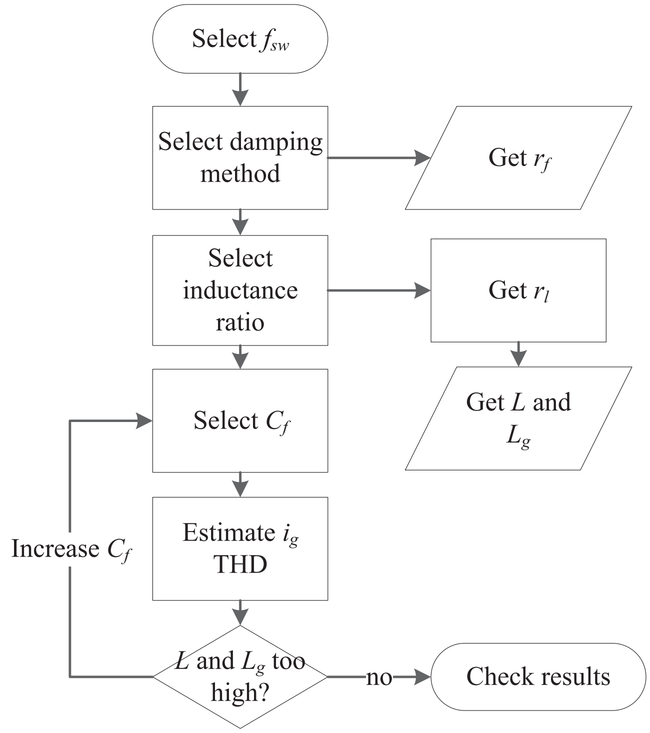

Fig. 5. Design flow for the *LCL*-filter.

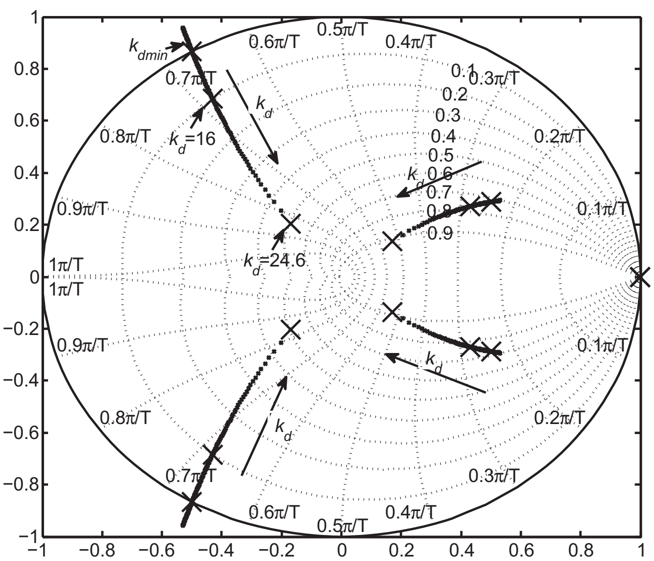

Fig. 6. Root locus in the *z*-plane for varying k_d.

V. Experimental Results

The parameters of the available experimental set-up are shown in TABLE I. The *DC*-link is supplied by a Delta Elektronika. A Danfoss FC302 converter is directly connected to the grid through an isolating transformer with the leakage inductance being L_g. For a system with the same switching frequency and capacitance, the design values for the converter and grid inductances, being $L = L_g = 1.5$ mH, are calculated

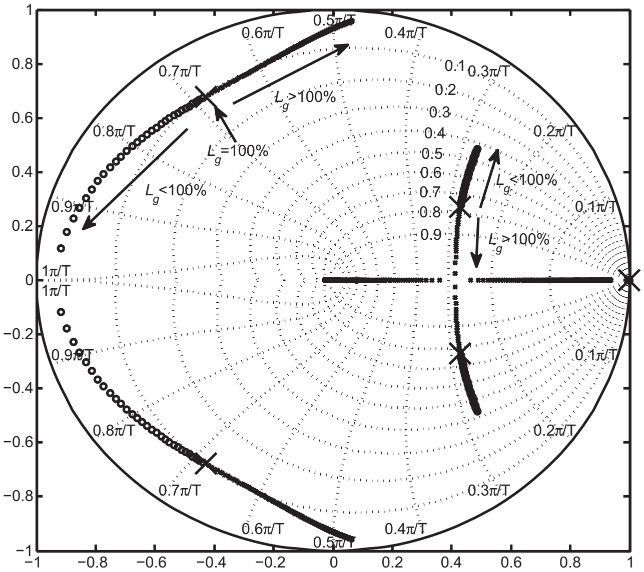

Fig. 7. Root locus in the z-plane for varying L_g from 40% to 1000%.

TABLE I
PARAMETERS OF THE EXPERIMENTAL SET-UP

Parameter	value
L	1.8 mH
C_f	4.7 μF
L_g	3 mH
$f_{sw}(= f_s)$	8 kHz
DC-voltage	650 V
Active power	2 kW
Reactive power	0 var

according to the proposed procedure. Thus, the real converter inductance is a little larger than the design value and the real grid inductance is almost double the design value. Notwithstanding that, the system remains stable upon the connection of the capacitor current feedback, as it is shown in Fig. 8.

To test the robustness of the proposed procedure, additional inductors of 6.9 mH are inserted between the converter and the isolated transformer. In this condition, without the capacitor current feedback, the grid converter trips. The experiment shown in Fig. 9 goes from inactive gate drivers (the capacitor current can be observed) to full rated generation. The system remains stable demonstrating the robustness of the proposed design procedure. The active damping method with the lead-lag network also results robust but not as much as with the capacitor current feedback. For this last experiment with the lead-lag method the grid converter does not trip but resonates considerably.

VI. CONCLUSIONS

A robust design procedure of *LCL*-filters for active damping in grid converters has been proposed in this paper. The proposed design flows require little iteration. The formulas for the resonance frequency, grid and converter inductance ratio and capacitance allows calculating all the needed parameters of the

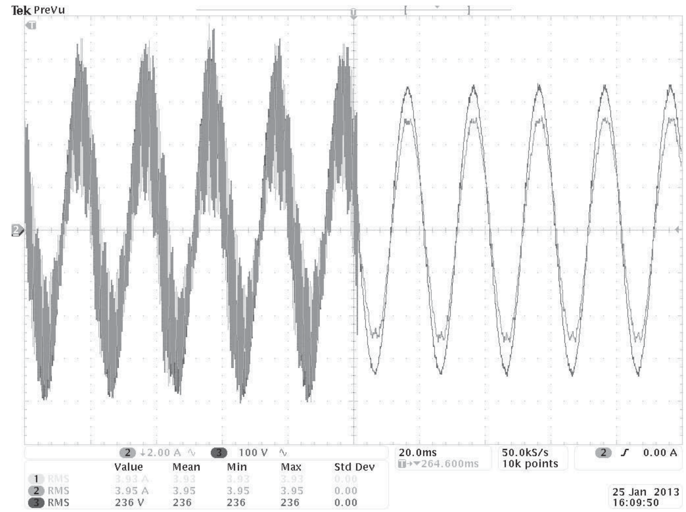

Fig. 8. Capacitor voltage and grid current upon the connection of the capacitor current feedback.

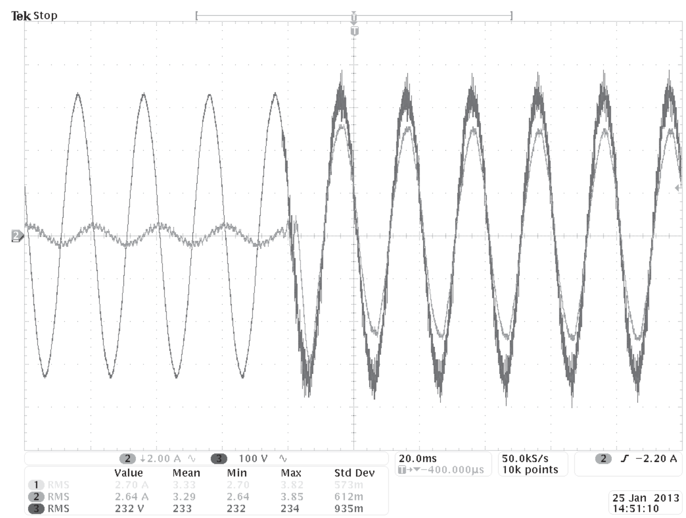

Fig. 9. Capacitor voltage and grid current from disconnection to connection of the *LCL*-filter based grid converter.

LCL-filter. The resultant designs demonstrate the significant robustness of the *LCL*-filter to grid inductance variations. This is especially the case of the capacitor current feedback, which allows selecting the damping of the resonance poles at will.

REFERENCES

[1] R. Teodorescu, M. Liserre, and P. Rodriguez, *Grid Converters for Photovoltaic and Wind Power Systems*. Wiley-IEEE Press, 2011.

[2] J. M. Guerrero, F. Blaabjerg, T. Zhelev, K. Hemmes, E. Monmasson, S. Jemei, M. P. Comech, R. Granadino, and J. I. Frau, "Distributed generation: Toward a new energy paradigm," *IEEE Ind. Electron. Mag.*, vol. 4, no. 1, pp. 52–64, Mar. 2010.

[3] M. Liserre, A. Dell'Aquila, and F. Blaabjerg, "Stability improvements of an LCL-filter based three-phase active rectifier," in *Proc. of PESC'02 - 33rd IEEE Annu. Power Electron. Specialists Conf.*, vol. 3, pp. 1195–1201, 2002.

[4] R. Peña-Alzola, M. Liserre, F. Blaabjerg, R. Sebastian, J. Dannehl, and F. W. Fuchs, "Analysis of the passive damping losses in LCL-filter-based grid converters," *IEEE Trans. Power Electron.*, vol. 28, no. 6, pp. 2642–2646, Jun. 2013.

[5] M. Liserre, F. Blaabjerg, and S. Hansen, “Design and control of an LCL-filter-based three-phase active rectifier,” *IEEE Trans. Ind. Appl.*, vol. 41, no. 5, pp. 1281–1291, Sept.-Oct. 2005.

[6] M. Orellana and R. Grino, “On the stability of discrete-time active damping methods for VSI converters with a LCL input filter,” in *Proc. of IECON 2012 - 38th Annu. Conf. IEEE Ind. Electron. Soc.*, pp. 2378–2383, Oct. 2012.

[7] R. Peña-Alzola, M. Liserre, F. Blaabjerg, R. Sebastian, J. Dannehl, and F. W. Fuchs, “Systematic design of the lead-lag network method for active damping in LCL-filter based three phase converters,” *IEEE Trans. Ind. Informatics*, accepted, 2013.

[8] M. Liserre, A. Dell’Aquila, and F. Blaabjerg, “Genetic algorithm-based design of the active damping for an LCL-filter three-phase active rectifier,” *IEEE Trans. Power Electron.*, vol. 19, no. 1, pp. 76–86, Jan. 2004.

[9] J. Dannehl, M. Liserre, and F. W. Fuchs, “Filter-based active damping of voltage source converters with LCL filter,” *IEEE Trans. Ind. Electron.*, vol. 58, no. 8, pp. 3623–3633, Aug. 2011.

[10] P. A. Dahono, “A method to damp oscillations on the input LC filter of current-type AC-DC PWM converters by using a virtual resistor,” in *Proc. of INTELEC’03 - 25th Int. Telecommun. Energy Conf.*, pp. 757–761, Oct. 2003.

[11] V. Blasko and V. Kaura, “A novel control to actively damp resonance in input LC filter of a three-phase voltage source converter,” *IEEE Trans. Ind. Appl.*, vol. 33, no. 2, pp. 542–550, Mar./Apr. 1997.

[12] J. Dannehl, F. W. Fuchs, S. Hansen, and P. B. Thogersen, “Investigation of active damping approaches for PI-based current control of grid-connected pulse width modulation converters with LCL filters,” *IEEE Tran. Ind. Appl.*, vol. 46, no. 4, pp. 1509–1517, Jul.-Aug. 2010.

[13] A. M. Hava, T. A. Lipo, and W. L. Erdman, “Utility interface issues for line connected PWM voltage source converters: a comparative study,” in *Proc. of APEC’95 - 10th Annu. Applied Power Electron. Conf. and Expo.*, vol. 1, no. 0, pp. 125–132, Mar. 1995.

[14] M. Liserre, R. Teodorescu, and F. Blaabjerg, “Stability of grid-connected PV inverters with large grid impedance variation,” in *Proc. of PESC’04 - 35th IEEE Annu. Power Electron. Specialists Conf.*, vol. 6, pp. 4773–4779, Jun. 2004.

[15] J. L. Agorreta, M. Borrega, J. Lopez, and L. Marroyo, “Modeling and control of N-paralleled grid-connected inverters with LCL filter coupled due to grid impedance in PV plants,” *IEEE Trans. Power Electron.*, vol. 26, no. 3, pp. 770–785, Mar. 2011.

[16] S. G. Parker, B. P. McGrath, and D. G. Holmes, “Regions of active damping control for LCL filters,” in *Proc. of ECCE’12 - IEEE Energy Conversion Congr. and Expo.*, pp. 53–60, Sept. 2012.

[17] V. Blasko and V. Kaura, “A new mathematical model and control of a three-phase AC-DC voltage source converter,” *IEEE Trans. Power Electron.*, vol. 12, no. 1, pp. 116–123, Jan. 1997.

[18] D. G. Holmes and T. A. Lipo, *Pulse Width Modulation for Power Converters:Principles and Practice*, 1st ed. Wiley-IEEE Press, 2003.

[19] S. Buso and P. Mattavelli, *Digital Control in Power Electronics*. Morgan and Claypool Publishers, 2006.

[20] G. F. Franklin, J. D. Powell, and M. L. Workman, *Digital Control of Dynamic Systems*. Addison-Wesley, 1997.

[21] P. Channegowda and V. John, “Filter optimization for grid interactive voltage source inverters,” *IEEE Trans. Ind. Electron.*, vol. 57, no. 12, pp. 4106–4114, Dec. 2010.

[22] M. Liserre, F. Blaabjerg, and A. Dell’Aquila, “Step-by-step design procedure for a grid-connected three-phase PWM voltage source converter,” *International Journal of Electronics*, vol. 91, no. 8, pp. 445–460, 2004.